Elastic scattering of electrons from F_2: An R-matrix calculation*

B. I. Schneider and P. J. Hay
Theoretical Division (T-6), Los Alamos Scientific Laboratory, Los Alamos, New Mexico 87545
(Received 26 January 1976)

The R-matrix method for electron-molecule scattering developed by one of us (B.I.S.) is applied to the elastic scattering of electrons from F_2 in the static-exchange approximation. Calculations are presented using both F_2 and F_2^- core orbitals to construct the electron-molecule interaction potential. The total and differential elastic scattering cross sections are quite different for the two molecular fields and can be interpreted in terms of the presence or absence of an F_2^- bound negative ion at the equilibrium internuclear separation in F_2. Since there is little experimental data on F_2^- or $e + F_2$ collisions, the calculations coupled with some detailed electron-beam experiments would be of great value in furthering our understanding of the chemistry of F_2^-.

I. INTRODUCTION

In the past four or five years there has been a rekindling of interest in the theory of electron-molecule collisions. Most of the early[1-5] work on electron-molecule scattering is based on the use of model potentials of one sort or another, with parameters chosen either from experiment or crude theoretical arguments. While these methods often give reasonable agreement with experiment, one can easily cite cases where they fail. What is perhaps even more important is that it is difficult, if not impossible, to rely on these theories as a predictive tool. Clearly what was needed was a well-founded theoretical model(s) based on the actual molecular structure of the system from which the cross sections could be computed in an *ab initio* fashion.

A great deal of progress along these lines was made in the late 1960's and early 1970's,[6-12] but it was not until 1974 that some new and quite general methods began to appear in the literature.[13-16] One of these techniques, the R-matrix method,[13,14] had been successfully applied to electron-atom collision problems by Burke and co-workers.[17] The extension of this method to multicenter scattering problems with nonspherical fields was not obvious. The essential step in the successful application of the R-matrix method to electron-molecule collisions was the introduction of an analytic basis set capable of accurately describing the scattering orbitals and yielding simple one- and two-electron matrix elements. Such a basis has been described by one of us in a previous publication.[14] The method has been applied to elastic $e + H_2$ scattering with considerable success, and its extension to treat both elastic and inelastic scattering, including polarization and short-range correlations, is in progress.

In this paper, we present an R-matrix calculation of $e + F_2$ elastic scattering in the static-exchange model. The calculation is significant for a variety of reasons. It is the first calculation of any sort on the scattering of electrons from F_2. Since F_2 is not a particularly spherical molecule, we would expect the coupling of partial waves to lead to reasonably large off-diagonal K-matrix elements at higher energies. This was borne out by the actual calculations above 8 eV incident energy.

The cross section shows a large potential or shape resonance at 1.8 eV. This resonance is in the P_σ wave and causes the cross section to rise to $130a_0^2$ at maximum.[18] One question we have tried to answer is whether this resonance is an artifact of the static-exchange approximation for F_2, or would it still be present in more sophisticated calculations. It is interesting to note that Fisk[2] in his 1937 paper predicted a low-energy resonance in $e + Cl_2$ collisions. In addition, he states that similar calculations of $e + F_2$ scattering give essentially identical results. The early experiments on the $e + Cl_2$ problem performed by Bailey and Healey[19] and Fisk[2] do show a resonance, but it is shifted to much higher energies and is considerably broader than in the calculated cross section. The experimental cross section is also much greater than the theoretical over the range of electron energies investigated.

Our greatest concern centers on the fact that the static-exchange field for F_2 does not support a bound negative ion at the F_2 equilibrium internuclear separation. The existence or nonexistence of a negative ion can have profound effects on the behavior of the scattering cross section. Since F_2 is such an electronegative gas, any calculational technique, *ab initio* or model potential based, could encounter severe difficulties. If F_2^- is bound at the F_2 internuclear distance, the resonance predicted by our calculation might well be the bound-state pole pushed into the continuum by a molecular field which is too weakly attractive.

Unfortunately, we cannot appeal to experiment to resolve the dilemma as there is little data available on F_2^- and no experimental cross sections are available for $e+F_2$ collisions. We have tried to settle the question by performing self-consistent-field (SCF) calculations on F_2^- at the F_2 internuclear distance. These calculations do indeed give a σ_u orbital bound by about 2 eV. Scattering calculations using the static-exchange field of F_2 but with F_2^- core orbitals do not show a resonance. This calculation is incorrect in the sense that the scattering is taking place off the wrong target state. However, it does show the dramatic effects of negative-ion formation on the behavior of the phase shifts. Hence we must conclude that the existence of the resonance depends quite critically on the presence or absence of an F_2^- bound ion at the equilibrium internuclear separation in F_2.

As our calculated cross sections for the two molecular fields are so different, there is little doubt that accurate beam data would resolve the difficulty. Consequently, we hope our theoretical results will be of sufficient interest to spur some experimental work on the $e+F_2$ problem. Since these cross sections are needed to model electron-beam initiated HF lasers, such results are of more than academic interest in laser-fusion–related research.

II. THEORY

Since the general technique has been presented in an earlier publication,[14] we give only those details necessary to understand the $e+F_2$ problem. The Hamiltonian for the scattering electron is (atomic units are used throughout the paper)

$$H=-\tfrac{1}{2}\nabla^2+V_N+2J-K, \tag{1a}$$

where

$$V_N=-Z\left[\frac{1}{r_{1a}}+\frac{1}{r_{1b}}\right], \quad 2J-K=\sum_{i=1}^{n}2J_i-K_i, \tag{1b}$$

and J_i and K_i are the Coulomb and exchange operators for the occupied F_2 orbitals ($1\sigma_g$, $1\sigma_u$, $2\sigma_g$, $2\sigma_u$, $3\sigma_g$, $1\pi_u$, $1\pi_g$). The orbitals were taken from SCF calculations on F_2 (case 1) and F_2^- (case 2) performed by the authors on the basis set described in Ref. 19. These orbitals were augmented by a set of diffuse s and p Gaussians on each center to form a representation of the interaction potential,

$$V=\sum_{\alpha,\beta}|\alpha\rangle\langle\alpha|V_N+2J-K|\beta\rangle\langle\beta|, \tag{2}$$

where $|\alpha\rangle$ refers to one member of an orthonormal set of molecular orbitals.

The orbital exponents for the diffuse functions were chosen in a geometric progression, the smallest exponent being 1.0×10^{-4}. The size of the basis set used to represent the potential was 82 functions of σ symmetry and 38 functions of π symmetry. In calculating the occupied π molecular orbitals for the σ-wave case, a contracted set of primitives was used. Similarly, for the π-wave case, a contracted set of σ orbitals was used to represent the occupied σ functions. The one-particle Hamiltonian was then diagonalized in the R-matrix basis. The box radius was chosen to be $\xi=10a_0$, well outside the charge distribution of F_2. From the eigenfunctions obtained in the diagonalization, we constructed the R matrix and extracted the K-matrix elements. Within the fixed-nuclei approximation the cross sections can be computed from the formulas given by Hara,[7]

$$\sigma=\frac{\pi}{k^2}\sum_{l,l',m}|T^m_{ll'}|^2, \tag{3a}$$

$$\frac{d\sigma}{d\Omega}=\frac{1}{k^2}\sum_{jl\lambda\mu m}\sum_{j'l'\lambda'\mu'm'}\sum_{L}X(jl\lambda\mu m)X^*(j'l'\lambda'\mu'm')\times\langle\lambda\lambda'-mm'|L-M_L\rangle\langle\mu\mu'm-m'|LM_L\rangle\langle\lambda\lambda'00|L0\rangle\langle\mu\mu'00|L0\rangle P_L(\cos\theta)/(2L+1), \tag{3b}$$

where

$$X(jl\lambda\mu m)=A_{j\lambda}A_{l\mu}[(\lambda+m)!(\mu+m)!/(\lambda-m)!(\mu-m)!]^{1/2}T^m_{jl}. \tag{3c}$$

The $A_{j\lambda}$ are the expansion coefficients for the spheroidal angular functions, S_{jm} in Legendre polynomials. The T^m_{jl} elements can be constructed from the K matrix and the total and differential cross sections computed from (3a) and (3b). A justification for the use of the fixed nuclei approximation can be found in Ref. 20.

III. CALCULATIONS

The calculational procedure is conveniently divided into the following parts:

(a) Choice of a primitive or contracted set of Gaussian atomic orbitals and evaluation of the one- and two-electron integrals.

TABLE I. Gaussian basis for SCF and static-exchange calculation, $\psi_i^c = X_c^{l_i} Y_c^{m_i} Z_c^{n_i} e^{-\alpha_i r_c^2}$.

α	l	m	n	α	l	m	n
9995.0	0	0	0	0.025	0	0	0
1506.0	0	0	0	0.015	0	0	0
350.3	0	0	0	0.0096	0	0	0
104.1	0	0	0	0.0060	0	0	0
34.84	0	0	0	0.0038	0	0	0
12.22	0	0	0	0.0023	0	0	0
4.369	0	0	0	0.0015	0	0	0
1.208	0	0	0	0.0001	0	0	0
0.3634	0	0	0	0.18	0	0	1
44.36	0	0	1	0.12	0	0	1
10.08	0	0	1	0.07	0	0	1
2.996	0	0	1	0.045	0	0	1
0.9383	0	0	1	0.028	0	0	1
0.2733	0	0	1	0.018	0	0	1
44.36	1	0	0	0.010	0	0	1
10.08	1	0	0	0.007	0	0	1
2.996	1	0	0	0.004	0	0	1
0.9383	1	0	0	0.0027	0	0	1
0.2733	1	0	0	0.0017	0	0	1
44.36	0	1	0	0.0010	0	0	1
10.08	0	1	0	0.000 65	0	0	1
2.996	0	1	0	0.18	1	0	0
0.9383	0	1	0	0.12	1	0	0
0.2733	0	1	0	0.07	1	0	0
0.90	0	0	2	0.045	1	0	0
0.90	0	2	0	0.028	1	0	0
0.90	2	0	0	0.018	1	0	0
0.90	1	1	0	0.010	1	0	0
0.90	1	0	1	0.007	1	0	0
0.90	0	1	1	0.004	1	0	0
				0.0027	1	0	0
				0.0017	1	0	0
0.10	0	0	0	0.0010	1	0	0
0.06	0	0	0	0.000 65	1	0	0
0.04	0	0	0				

(b) Calculation of the occupied molecular orbitals of F_2 or F_2^- in the basis defined in (a) using the Hartree-Fock SCF procedure. The functions used to describe the occupied orbitals are the $9s5p$ primitive bases of Huzinaga[19] augmented by a set of $3d$ polarization functions. For the σ-wave calculation, the fluorine π functions (p_x and p_y) were contracted to two functions. Similarly, for the π-wave calculations, the s and p_z σ functions were contracted to $3s$ and $2p$ functions, respectively.

(c) Calculation of the Hartree-Fock virtual orbitals of F_2 or F_2^- using the occupied orbitals obtained from step (b). The use of a completely contracted basis was found to provide too few virtual orbitals to describe the interaction potential in Eq. (2) adequately. Hence a completely uncontracted basis was used to describe the virtual F_2 or F_2^- orbitals. No bound (negative energy) virtual orbitals were found in the SCF calculation of F_2 at the experimental bond distance of 1.42Å. When F_2^- orbitals were used to construct the Hamiltonian in (1a), one bound virtual orbital of $3\sigma_u$ symmetry was obtained with an orbital energy of 2 eV.

(d) Transformation of the Hartree-Fock potential from the atomic Gaussian orbitals to the set of occupied and virtual molecular orbitals.

(e) Choice of the R-matrix basis and transformation of the Hartree-Fock potential to this basis via the equation

$$(\psi_i | V | \psi_j) = \sum_{\alpha,\beta} (\psi_i | \alpha) V_{\alpha\beta} (\beta | \psi_j). \tag{4}$$

As we pointed out in Ref. 13, the use of two basis sets allows us to calculate the difficult two-electron integrals $V_{\alpha\beta}$ with standard integral programs such as POLYATOM.[21] A simple transformation requiring only overlap integrals on the finite interval gives us the needed potential matrix elements

TABLE II. R-matrix basis for static-exchange calculations in F_2 [see Eq. (5) and accompanying text].

α	β	l	m	A	α	β	l	m	A
0.001	0.0001	0	0	0.0	4.0	−2.0	0	0	2.0
0.001	−0.0001	0	0	0.0	2.0	4.0	0	0	2.0
0.001	0.0001	1	1	0.0	2.0	−4.0	0	0	2.0
0.001	−0.0001	1	1	0.0	5.0	3.0	0	0	2.0
0.001	0.0001	2	2	0.0	5.0	−3.0	0	0	2.0
0.001	−0.0001	2	2	0.0	1.0	1.0	1	1	2.0
0.001	0.0001	3	3	0.0	1.0	−1.0	1	1	2.0
0.001	−0.0001	3	3	0.0	2.0	2.0	1	1	2.0
10.0	10.0	0	0	0.0	2.0	−2.0	1	1	2.0
10.0	−10.0	0	0	0.0	2.0	2.0	0	0	4.0
4.0	4.0	0	0	0.0	2.0	−2.0	0	0	4.0
4.0	−4.0	0	0	0.0	1.0	1.0	0	0	4.0
2.0	2.0	0	0	0.0	1.0	−1.0	0	0	4.0
2.0	−2.0	0	0	0.0	4.0	2.0	0	0	4.0
1.0	1.0	0	0	0.0	4.0	−2.0	0	0	4.0
1.0	−1.0	0	0	0.0	2.0	4.0	0	0	4.0
8.0	5.0	0	0	0.0	2.0	−4.0	0	0	4.0
8.0	−5.0	0	0	0.0	5.0	3.0	0	0	4.0
5.0	8.0	0	0	0.0	5.0	−3.0	0	0	4.0
5.0	−8.0	0	0	0.0	1.0	1.0	1	1	4.0
4.0	2.0	0	0	0.0	1.0	−1.0	1	1	4.0
4.0	−2.0	0	0	0.0	2.0	2.0	1	1	4.0
1.0	3.0	0	0	0.0	2.0	−2.0	1	1	4.0
1.0	−3.0	0	0	0.0	2.0	2.0	0	0	6.0
5.0	3.0	0	0	0.0	2.0	−2.0	0	0	6.0
5.0	−3.0	0	0	0.0	4.0	1.0	0	0	6.0
3.0	5.0	0	0	0.0	4.0	−1.0	0	0	6.0
3.0	−5.0	0	0	0.0	4.0	2.0	0	0	6.0
4.0	4.0	1	1	0.0	4.0	−2.0	0	0	6.0
4.0	−4.0	1	1	0.0	2.0	4.0	0	0	6.0
2.0	2.0	1	1	0.0	2.0	−4.0	0	0	6.0
2.0	−2.0	1	1	0.0	5.0	3.0	0	0	6.0
1.0	1.0	1	1	0.0	5.0	−3.0	0	0	6.0
1.0	−1.0	1	1	0.0	1.0	1.0	1	1	6.0
8.0	5.0	1	1	0.0	1.0	−1.0	1	1	6.0
8.0	−5.0	1	1	0.0	2.0	2.0	1	1	6.0
2.0	4.0	1	1	0.0	2.0	−2.0	1	1	6.0
2.0	−4.0	1	1	0.0	4.0	2.0	1	1	6.0
6.0	2.0	1	1	0.0	4.0	−2.0	1	1	6.0
6.0	−2.0	1	1	0.0	5.0	8.0	1	1	6.0
3.0	5.0	1	1	0.0	5.0	−8.0	1	1	6.0
3.0	−5.0	1	1	0.0	0.5	0.5	1	1	2.0
2.0	2.0	0	0	2.0	0.5	−0.5	1	1	2.0
2.0	−2.0	0	0	2.0	0.5	0.5	1	1	4.0
1.0	1.0	0	0	2.0	0.5	−0.5	1	1	4.0
1.0	−1.0	0	0	2.0	0.5	0.5	1	1	6.0
4.0	2.0	0	0	2.0	0.5	−0.5	1	1	6.0

for the R-matrix calculation.

(f) Diagonalization of the static-exchange Hamiltonian in the R-matrix basis.

(g) Construction of the R matrix using the eigenfunctions obtained from step (f).

(h) Numerical integration from infinity to the R-matrix surface, including any long-range multipole potentials in each channel and the solution of a set of algebraic equations of dimension of the number of channels needed to describe the scattering, to obtain the K-matrix elements. The permanent quadrupole moment of F_2 computed with our basis set is $0.60a_0^2$ in excellent agreement with the experimental value of $0.65a_0^2$. Inclusion of the contribution of this long-range potential in the external region had little effect on our results. Presumably this is a consequence of the small size of the permanent quadrupole moment in F_2.

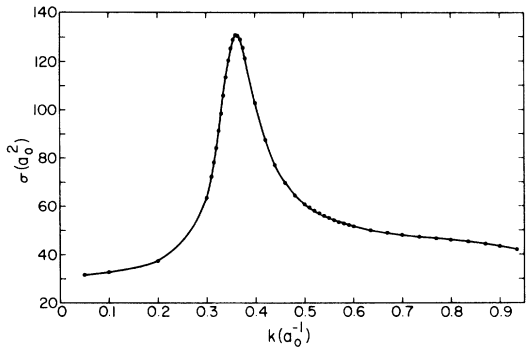

FIG. 1. Total elastic cross section for $e + F_2$ scattering (F_2 core orbitals).

(i) Calculation of total and differential cross sections using Eqs. (3a)–(3c).

The basis set of primitives used in the first and second steps is given in Table I. The functions appearing above the dashed line were used to compute the occupied orbitals. The R-matrix basis used to diagonalize the static-exchange Hamiltonian was constructed from a set of elliptic floating Gaussians of the form

$$\Phi_i(\xi,\eta,\phi) = \xi^{l_i}\eta^{m_i}[(\xi^2-1)(1-\eta^2)]^{\nu_i/2} \times e^{-\beta_i r}e^{-\alpha_i(\xi-A_i)^2}\begin{Bmatrix}\sin\nu_i\phi\\ \cos\nu_i\phi\end{Bmatrix}. \quad (5)$$

The values of the parameters l, m, β, α, and A appear in Table II. The most time-consuming steps of the calculation are steps (a)–(d). The diagonalization of the Hamiltonian and the extraction of the K-matrix elements at 47 energies took an order of magnitude less time than steps (a)–(d). This allowed us to study the behavior of the cross section around the resonance in great detail and is one of the great advantages of the R-matrix method.

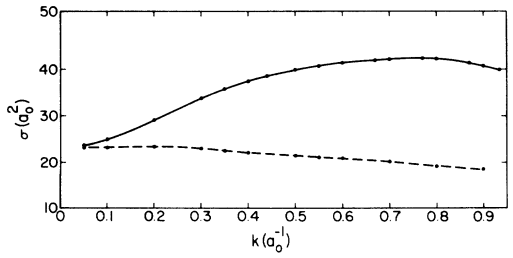

FIG. 2. Solid curve: total elastic cross section for $e + F_2$ scattering (F_2^- core orbitals). Dashed curve: momentum transfer cross section for $e + F_2$ scattering (F_2^- core orbitals).

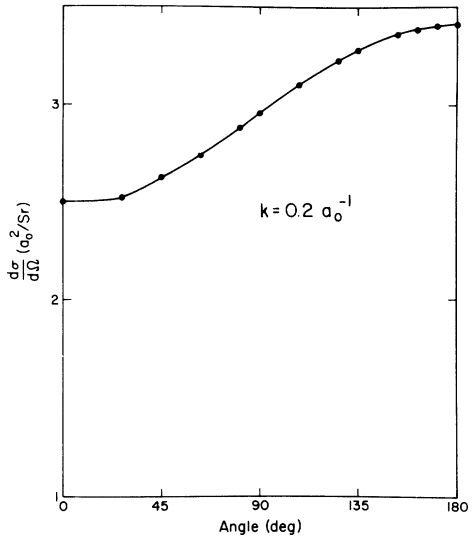

FIG. 3. Differential cross section for $e + F_2$ scattering at $k = 0.2a_0^{-1}$ (F_2 core orbitals).

IV. NUMERICAL RESULTS

The calculations described in Sec. III have been carried out for σ and π symmetry using both F_2 and F_2^- core orbitals. Six partial waves were retained in the external region and in the matching step. Since the internal basis set was chosen to describe s, p, and d partial waves accurately, we did not use the phase shifts for higher l values in calculating the cross sections reported in this paper. However, we did examing the f partial waves and found them to be considerably smaller than the d-wave contribution. Calculations including f-wave contributions were performed at isolated energies; these contributions were found to have a negligible effect on the cross sections. As

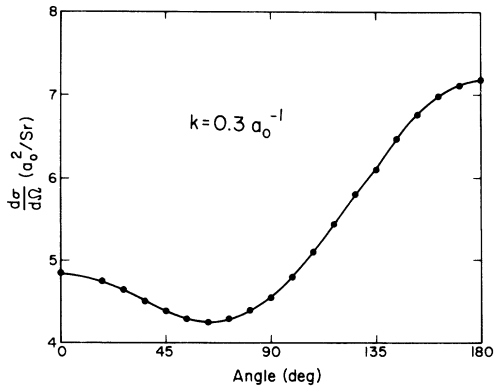

FIG. 4. Same as for Fig. 3, but at $k = 0.3a_0^{-1}$.

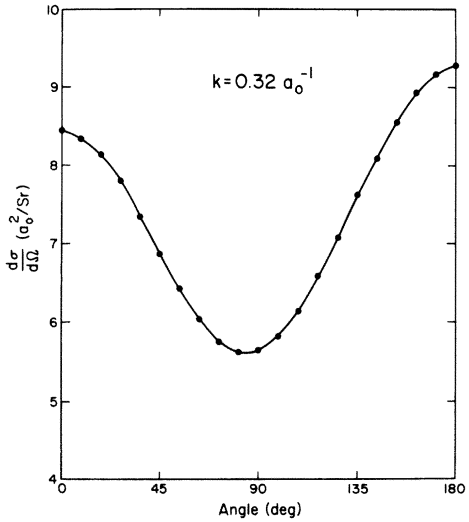

FIG. 5. Same as for Fig. 3, but at $k=0.32a_0^{-1}$.

is quite evident from Figs. 1 and 2, the nature of the scattering is qualitatively different for the molecular field based on F_2 or F_2^- core orbitals. The reason for this is quite simple. The static-exchange potential used in most scattering calculations is constructed from a wave function of the form

$$\psi = \mathcal{A}(\theta_T \chi), \tag{6a}$$

where

$$\theta_T = \mathcal{A}(\Psi_1 \cdots \Psi_N). \tag{6b}$$

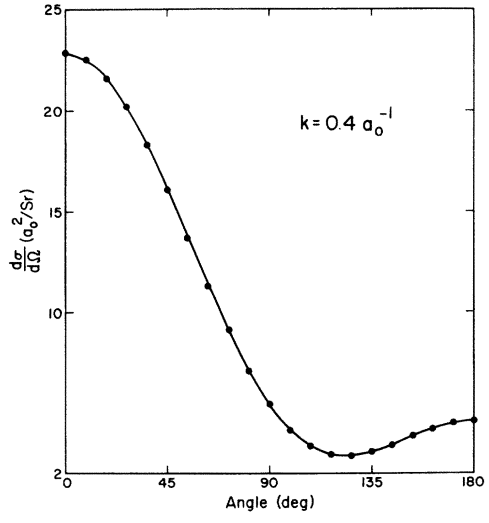

FIG. 6. Same as for Fig. 3, but at $k=0.4a_0^{-1}$.

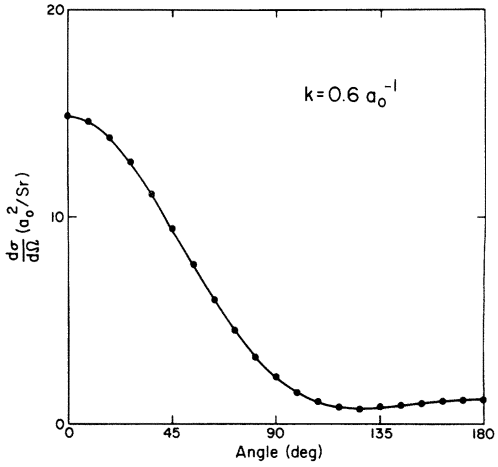

FIG. 7. Same as for Fig. 3, but at $k=0.6a_0^{-1}$.

The molecular orbitals of the target, $\Psi_1 \cdots \Psi_N$, are calculated in the Hartree-Fock potential for N rather than $N+1$ electrons. Consequently, if a true negative ion of the $(N+1)$-electron system exists, it will not be described correctly, if at all, in this potential. For the $e+F_2$ system, the static-exchange field based on unperturbed F_2 orbitals does not give a bound F_2^- ion at the equilibrium internuclear separation in F_2. Hartree-Fock calculations on the compound system, on the other hand, do produce a bound negative ion. The scattering from these two potentials is quite different. When the potential does not support a bound-negative-ion state, we find a large P_σ shape resonance at 1.8 eV. The differential cross section (see Figs. 3–8) changes drastically as a function of

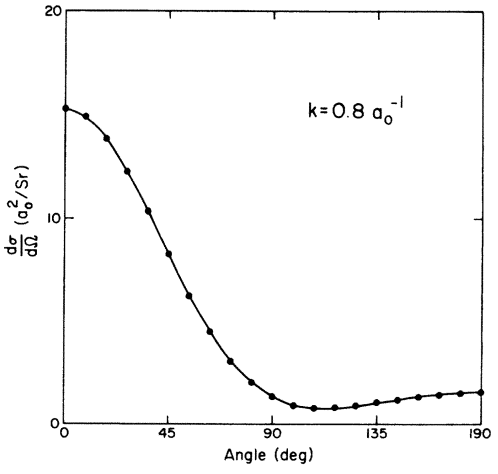

FIG. 8. Same as for Fig. 3, but at $k=0.8a_0^{-1}$.

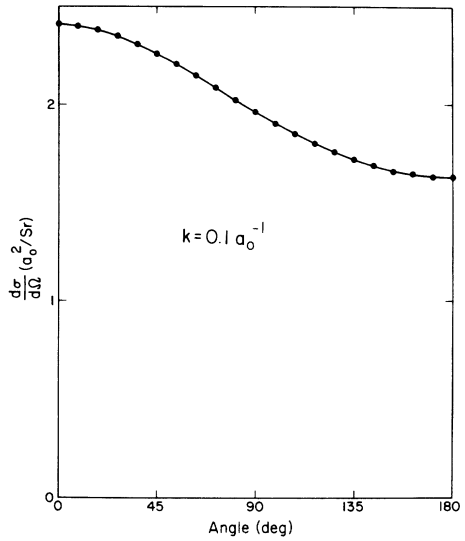

FIG. 9. Same as for Fig. 3, but at $k = 0.1a_0^{-1}$ and for F_2^- core orbitals.

energy from backward peaking at small k to forward peaking at high k. Near the resonance we expect a cosinelike behavior and, indeed, we see this in Fig. 5. The same potential using F_2^- orbitals does support a negative ion and shows no resonance behavior in any of the eigenphases or cross sections. The differential cross section is forward peaked at all k (see Figs. 9–13), typical of a scattering situation dominated by direct rather than exchange forces. In short, our resonance pole has moved to the negative real axis, and this has profound consequences on the nature of the scattering cross section. For completeness, we present the momentum transfer cross section for electrons on F_2 in the dashed curve in Fig. 2.

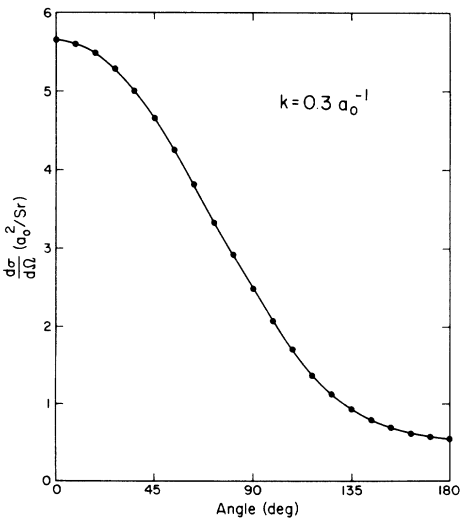

FIG. 10. Same as for Fig. 9, but at $k = 0.3a_0^{-1}$.

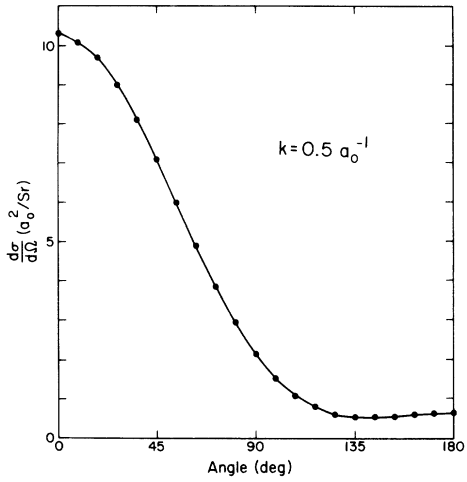

FIG. 11. Same as for Fig. 9, but at $k = 0.5a_0^{-1}$.

It is interesting to make some qualitative comparisons between our results for F_2 and the known cross sections for electron impact on N_2 and O_2.[22] Since N_2 does not support a bound negative ion, we would expect the shape of its cross section to resemble our case 1. This is indeed the case, with N_2 showing a large resonance around 2–2.5 eV. The cross section at the peak of the resonance is $100–110a_0^2$, in agreement with our value of $130a_0^2$ for F_2. O_2, on the other hand, does support a negative ion and shows no obvious resonant behavior in its cross section aside from the well-known vibrational resonances associated with the bound O_2^- state. The shape and magnitude of the cross section are in qualitative agreement with case 2 in F_2. Although long-range polarization would have some effect on the quantitative details

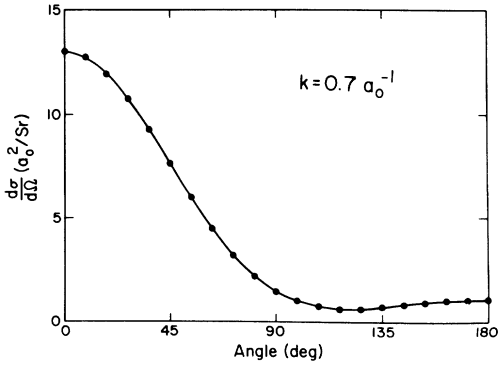

FIG. 12. Same as for Fig. 9, but at $k = 0.7a_0^{-1}$.

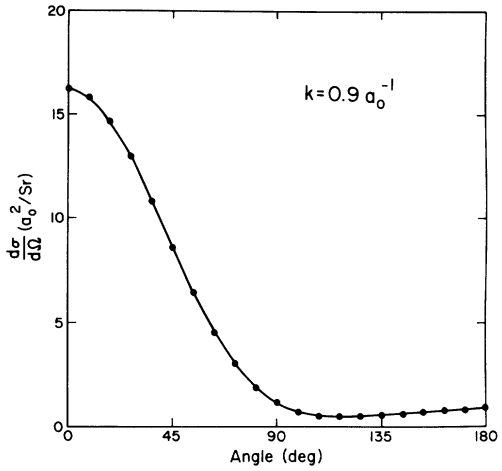

FIG. 13. Same as for Fig. 9, but at $k = 0.9a_0^{-1}$.

of the cross section, the qualitative picture we have just described should be unchanged.

The experimental situation is less satisfactory than one would hope for. There is no information on the existence of a bound negative F_2^- ion at the equilibrium internuclear distance in F_2, although F_2^- is probably more stable than F_2 at its own equilibrium internuclear separation. The corrosive nature of fluorine has put off experimentalists, and the elastic scattering cross section has never been measured in spite of its importance in understanding electron-beam–initiated fluoride lasers. The authors hope the theoretical calculations presented in this paper will stimulate the experimentalists to measure some of these quantities. A careful electron-beam study of $e + F_2$ collisions would bring a great deal of understanding to the chemistry of F_2 and its negative ion.

*Work performed under the auspices of the U. S. Energy Research and Development Administration.

[1]H. C. Stier, Z. Phys. 76, 439 (1932).
[2]J. B. Fisk, Phys. Rev. 49, 167 (1936); 51, 25 (1937).
[3]The importance of exchange was first pointed out by H. S. W. Massey and R. O. Ridley, Proc. Phys. Soc. (Lond.) A 69, 659 (1956). This calculation used the Kohn variational principle with a simple trial wave function.
[4]C. Carter, N. H. March, and D. Vincent, Proc. Phys. Soc. (Lond.) 71, 2 (1958).
[5]S. Nagahara, J. Phys. Soc. Jpn. 8, 165 (1953); 9, 52 (1954).
[6]N. F. Lane and R. J. W. Henry, Phys. Rev. 183, 221 (1969).
[7]S. Hara, J. Phys. Soc. Jpn. 27, 1009 (1969).
[8]A. Temkin and K. V. Vasavada, Phys. Rev. 160, 109 (1967).
[9]J. C. Tully and R. S. Berry, J. Chem. Phys. 51, 2056 (1969).
[10]P. G. Burke and A. L. Sinfailam, J. Phys. B 3, 641 (1970).
[11]P. G. Burke and N. Chandra, J. Phys. B 5, 1696 (1972).
[12]P. G. Burke, N. Chandra, and F. A. Gianturco, J. Phys. B 5, 2212 (1972).
[13]B. Schneider, Chem. Phys. Lett. 31, 237 (1975).
[14]B. Schneider, Phys. Rev. 11, 1957 (1975).
[15]T. N. Rescigno, C. W. McCurdy, and V. McKoy, Chem. Phys. Lett. 27, 401 (1974).
[16]T. N. Rescigno, C. W. McCurdy, and V. McKoy, Phys. Rev. 11, 825 (1975).
[17]P. G. Burke, A. Hibbert, and W. D. Robb, J. Phys. B 4, 153 (1971).
[18]At very low energies, including that of the resonance, the eigenphases are totally dominated by a single partial wave.
[19]V. A. Bailey and R. H. Healey, Philos. Mag. 19, 725 (1935).
[20]D. E. Golden, Neal F. Lane, A. Temkin, and E. Gerjoy, Rev. Mod. Phys. 43, 642 (1971).
[21]A description of POLYATOM and a copy of the program can be obtained from the Quantum Chemistry Program Exchange, University of Indiana, Bloomington, Indiana.
[22]L. J. Kieffer, *A Compilation of Electron Collision Cross Section Data for Modeling Gas Discharge Lasers*, JILA Information Center report No. 13 (University of Colorado, Boulder, Col.) (unpublished).